Continental Shelf Research 72 (2014) 73–82

Contents lists available at ScienceDirect

Continental Shelf Research

journal homepage: www.elsevier.com/locate/csr

Research papers

Shoreline dissipation of infragravity waves

A.T.M. de Bakker*, M.F.S. Tissier, B.G. Ruessink

Department of Physical Geography, Faculty of Geosciences, Utrecht University, P.O. Box 80115, 3508 TC Utrecht, The Netherlands

ARTICLE INFO

Article history:
Received 20 December 2012
Received in revised form
24 September 2013
Accepted 13 November 2013
Available online 20 November 2013

Keywords:
Infragravity waves
Energy flux
Reflection
Dissipation
Wave breaking

ABSTRACT

Infragravity waves (0.005–0.05 Hz) have recently been observed to dissipate a large part of their energy in the short-wave (0.05–1 Hz) surf zone, however, the underlying mechanism is not well understood. Here, we analyse two new field data sets of near-bed pressure and velocity at up to 13 cross-shore locations in $\lesssim$2.5 m depth on a $\approx 1:80$ and a $\approx 1:30$ sloping beach to quantify infragravity-wave dissipation close to the shoreline and to identify the underlying dissipation mechanism. A frequency-domain Complex Eigenfunction analysis demonstrated that infragravity-wave dissipation was frequency dependent. Infragravity waves with a frequency larger than $\approx$0.0167–0.0245 Hz were predominantly onshore progressive, indicative of strong dissipation of the incoming infragravity waves. Instead, waves with a lower frequency showed the classic picture of cross-shore standing waves with minimal dissipation. Bulk infragravity reflection coefficients at the shallowest position (water depth $\approx$0.7 m) were well below 1 ($\approx$0.20), implying that considerable dissipation took place close to the shoreline. We hypothesise that for our data sets infragravity-wave breaking is the dominant dissipation mechanism close to the shoreline, because the reflection coefficient depends on a normalised bed slope, with the higher infragravity frequencies in the mild-sloping regime where breaking is known to dominate dissipation. Additional numerical modelling indicates that, close to the shoreline of a 1:80 beach, bottom friction contributes to infragravity-wave dissipation to a limited extent, but that non-linear transfer of infragravity energy back to sea–swell frequencies is unimportant.

1. Introduction

Infragravity waves are 20–200 s motions in the ocean surface that are strongest near the shore, and may be responsible for beach (e.g. Russell, 1993) and dune (Van Thiel de Vries et al., 2007) erosion. Infragravity waves can arise from the non-linear energy transfer from $<$20 s sea and swell waves. In deep water the transfer of energy is non-resonant and the height of infragravity waves is a few millimeters at most. In coastal and nearshore water depths the energy transfer becomes near-resonant and, as a consequence, infragravity-wave height can increase rapidly to over 1 m (e.g. Guza and Thornton, 1982; Ruessink et al., 1998; Sénéchal et al., 2011). During the breaking of the sea and swell waves, the infragravity waves propagate towards the beach as free waves and reflect from the shoreline. The simultaneous presence of shoreward propagating and reflected infragravity waves gives rise to a standing wave pattern (Guza and Thornton, 1985).

The predominantly observed cross-shore standing nature implies that infragravity-wave dissipation in the sea–swell surf zone must generally be small. Interestingly, Guza and Thornton (1985) observed infragravity frequencies above 0.03 Hz to show an increasingly progressive wave pattern, suggesting some infragravity-wave dissipation. The (crudely estimated) infragravity-wave reflection coefficient, the ratio of seaward to shoreward propagating infragravity-wave energy flux, of 0.5 confirms this. Other observations indicate (bulk, i.e. frequency integrated) infragravity-wave dissipation to be considerably higher. For example, Ruessink (1998b) observed the infragravity wave-height to decrease rather than to increase onshore in the surf zone of a low-sloping ($\approx 1:200$) multiple barred system. For the same site, Ruessink et al. (1998) found swash spectra to saturate well into the infragravity band, indicative of energy dissipation due to infragravity-wave breaking. Later, saturation at infragravity frequencies was also observed at other sites (Ruggiero et al., 2004; Sénéchal et al., 2011; Guedes et al., 2013).

Since these initial observations, several infragravity-wave dissipation mechanisms have been suggested in the literature. Henderson and Bowen (2002) mentioned bottom friction as the dominant mechanism; however, the implied drag coefficient in the bottom friction formulation is unrealistically high for sandy beaches (Henderson et al., 2006). For coral reefs, bottom friction does play a dominant role in the energy dissipation of infragravity waves, as the friction coefficient is an order of magnitude larger, $c_f \approx$ 0.02–0.05, than on sandy beaches where $c_f \approx 0.005$ is already quite high (Pomeroy et al., 2012; Van Dongeren et al., 2013).

* Corresponding author. Tel.: +31 30 253 7453; fax: +31 30 253 1145.
E-mail address: a.t.m.debakker@uu.nl (A.T.M. de Bakker).

0278-4343/$ - see front matter © 2013 Elsevier Ltd. All rights reserved.
http://dx.doi.org/10.1016/j.csr.2013.11.013

Instead, Henderson et al. (2006) suggested the existence of non-linear energy transfer back to sea–swell frequencies through triad interactions, as did Thomson et al. (2006) and Guedes et al. (2013). Thomson et al. (2006) show this non-linear transfer to be particularly relevant in the inner surf zone in water depths larger than about 1 m, where sea–swell energy still dominates over infragravity energy. Closer to the shore, their incoming and outgoing infragravity fluxes were about equal, suggesting minimal infragravity-wave dissipation at the shoreline. Instead, Battjes et al. (2004) and Van Dongeren et al. (2007) observed dissipation to be strongest at a laboratory shoreline and suggested that infragravity-wave breaking played a role. The concept of infragravity-wave breaking is supported by Lin and Hwung (2012), who performed high-resolution laboratory experiments over varying (1:10–1:60) sloping beds. Furthermore, Nazaka and Hino (1991) observed infragravity waves on a laboratory reef to possess a bore-like shape, similar to breaking sea–swell waves.

Based on the work of Battjes (1974), Van Dongeren et al. (2007) found that the shoreline amplitude reflection coefficient R of monochromatic infragravity waves is related to a normalized bed slope, β_H, as $R = 2\pi\beta_H^2$, with

$$\beta_H = \frac{\beta T}{2\pi}\sqrt{\frac{g}{H^+}}. \quad (1)$$

Here, β is the bed slope, H^+ is the height of the incoming infragravity wave with period T, and $g = 9.81$ m/s^2 is the gravitational acceleration. This parameter is based on the concept that a given bed slope appears steeper to longer (lower frequency) waves than it does to shorter (higher frequency) waves. On a steeper slope, more energy will be reflected (i.e. less energy will be dissipated). Van Dongeren et al. (2007) delineated a mild-sloping regime ($\beta_H < 1.25$) where energy is dissipated by infragravity-wave breaking, from a steep-sloping regime ($\beta_H > 1.25$) where $R \approx 1$ and almost no infragravity-wave energy dissipates. The transition at approximately $\beta_H = 1.25$ is similar to the value previously found for the onset of short wave breaking (Battjes, 1974). Additionally, Van Dongeren et al. (2007) showed that in the infragravity breaking-zone the dominant triad interactions are infragravity self–self interactions, rather than the infragravity sea–swell interactions investigated by Henderson et al. (2006), Thomson et al. (2006) and Guedes et al. (2013). Recently, Ruju et al. (2012) suggested, based on a numerical evaluation of the radiation stresses and the infragravity-wave energy balance, that both breaking and non-linear energy transfer could play a role, each mechanism in another water depth range within the short-wave surf zone. Seaward of the inner short-wave surf zone where short waves still dominate over infragravity waves, the infragravity waves transferred their energy back to the short waves through triad interactions, while in the inner surf zone the remaining infragravity energy was most likely dissipated due to infragravity-wave breaking. Despite the extensive modelling work, laboratory- and field experiments that have been devoted to identifying the possible sources of infragravity energy loss, the exact infragravity-dissipation mechanism(s) is(are) still unclear and most process-based models do not account for the significant infragravity-wave dissipation observed in the field.

Here, we present field observations of infragravity waves from two field sites contrasting in beach slope with the specific focus on the shoreline dissipation source. In this way, we extend the primarily laboratory (Van Dongeren et al., 2007) and modelling based work (Ruju et al., 2012) on infragravity-wave breaking. In Section 2 we describe the data sets, and introduce our analysis methods. The results and the likely relevance of infragravity-wave breaking to inshore dissipation are described in Section 3. In Section 4, we examine the role of both bottom friction and non-linear energy transfer in infragravity dissipation using numerical modelling. Furthermore, we here elaborate the effect of beach slope on infragravity-wave reflection. Our main results are summarized in Section 5.

2. Methods

2.1. Field site and instruments

Field observations of near-bed pressure and velocity were collected during two field campaigns in the Netherlands. The first campaign was carried out during autumn 2010, on the low-sloping North Sea facing Ballum beach ($\approx 1:80$) on the barrier island Ameland (Ruessink et al., 2012). The second field campaign took place during autumn 2011 on the steeper-sloping Egmond beach ($\approx 1:20$–$1:40$). During both field experiments, instruments were placed in a cross-shore array in the intertidal zone. The arrays extended from the low-tide spring level (1 m below Mean Sea Level, MSL) to the high-tide level that is expected for a typical autumn storm coinciding with spring tide (1.5 m above MSL), see Fig. 1. Along each transect 9 pressure transducers (PTs) were placed that sampled continuously at 5 Hz. At three locations, in between these PTs, electromagnetic flowmeters (EMFs) and other PTs were co-located, sampling continuously at 4 Hz. Additionally, the Ameland array comprised a rig equipped with a PT (sampling frequency of 4 Hz) and three Sontek Acoustic Doppler Velocimeter Ocean (ADVO) probes (sampling frequency of 10 Hz). The ADVO probes were placed in a vertical array (PT5 at Ameland) to study surf zone turbulence (Grasso and Ruessink, 2012) (Fig. 1). During both deployments, the array thus comprised 12 (Egmond) or 13 (Ameland) instrumented positions, all with PTs and three (Egmond) or four (Ameland) positions with equipment to measure flow velocities. The PTs were positioned at around 5–10 cm above the bed; the EMFs were repositioned every day to a height of about 20 cm above the bed. The transect was measured several times with a Differential Global Positioning System (DGPS) during the Ameland campaign, and daily at Egmond because of the higher morphological variability (see Fig. 1). The bed material had a median grain size of about 200 μm and 300 μm on Ameland and Egmond, respectively.

2.2. Initial data processing

At both sites, data were collected for approximately six weeks. For each tide, a block of 2 h of data centred around high tide was selected. During these two hours, wave statistics (height, period) and the water level were approximately stationary. The data were corrected for small (< 1 s/day) clock drifts. The pressure data were converted to free surface elevation, with a depth correction using linear wave theory. When part of the data at a specific location showed intermittently dry and wet conditions, the entire series was removed. Thus, all data analysed here were collected seaward of the swash zone. As we focus on cross-shore infragravity dynamics, two selection methods were defined regarding alongshore low-frequency

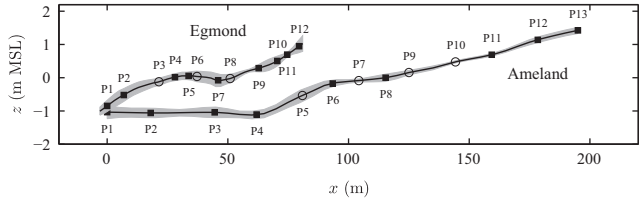

Fig. 1. The campaign-mean bed elevation z with respect to MSL versus cross-shore distance x for both Ameland and Egmond. The gray region is the bathymetry standard deviation over time. Black filled squares indicate the PTs, open circles indicate collocated flow meters and PTs.